Shock-induced molecular excitation in solids

Frank J. Zerilli and Edward T. Toton*

Naval Surface Weapons Center, U.S. Department of the Navy, White Oak, Silver Spring, Maryland 20910

Initiation of condensed explosives is studied on a molecular level with a quantum-mechanical calculation of transition rates for shock-induced transitions between the low-lying internal molecular normal-mode states in a molecular solid. It is assumed that the shock produces a distribution of acoustic phonons which become thermalized before any significant number of internal-mode phonons is created. The calculation uses the Born-Oppenheimer approximation in which the internal modes constitute the fast subsystem and the acoustic modes the slow subsystem. A sample calculation is done for nitromethane. Generally speaking, the lowest-frequency internal modes have the fastest shock-induced transition (highest rates), with the transition from the ground to first excited state being the slowest. The transition rates increase by 6 to 10 orders of magnitude from the values under normal conditions when nitromethane is subjected to shocks of 50 to 300 kbar. The transition lifetimes are compared with, and show some correlation with, the pressure-time critical-shock initiation data obtained by de Longueville, Fauquignon, and Moulard.

I. INTRODUCTION

The motivation for this work is to understand the early phase of the initiation of condensed explosives on a molecular level. For this purpose, nonradiative transition rates are calculated for shock-induced transitions between the low-lying internal-normal-mode states in a molecular lattice in an attempt to understand how the energy from a shock wave is transferred to the internal molecular modes.

Pastine and co-workers pointed out that because many explosives have weak intermolecular bonds and strong covalent intramolecular bonds the average frequency of intramolecular (internal-mode or optical-mode) vibrations ω_0 would be much higher than the average frequency of intermolecular (lattice-mode or acoustic-mode) vibrations ω_a with the ratio ω_0/ω_a typically of the order of 10.[1] Thus the immediate effect of a shock on such materials would be to increase the temperature of the acoustic vibrational branch while leaving the optical branches at the initial temperature. The relaxation time required before the internal molecular temperature reaches a critical value sufficient for the shock to grow to detonation would be sufficiently long so as to be comparable to and indeed determine the shock pulse duration required to produce detonation at a given shock pressure. In other words, the relaxation time for thermal equilibration of the internal modes is the controlling factor in the initiation of reactions. With the use of a simple classical mass and spring model, Pastine et al. estimated that, at a shock temperature of 500 K, the lower limit to the acoustic-optical relaxation time is of the order of several microseconds for systems in which the acoustic frequencies ω_a are around 10^{13} rad/sec and the optical-mode frequencies ω_0 are around 10^{14} rad/sec. They also predicted that the relaxation times would be very sensitive functions of the frequency ratio ω_0/ω_a with the relaxation times decreasing by 4 orders of magnitude when the ratio decreases from 10 to 6. Thus the very lowest-frequency intramolecular

modes, which are typically bending rather than stretching modes, should be the most important in the relaxation process.

Later, Toton developed a more refined quantum-mechanical description which exploited the disparity between the intramolecular- and intermolecular-mode vibrational frequencies.[2] The results of Toton's calculations also pointed toward the importance of the lowest-frequency intramolecular modes in the relaxation process. Here we develop Toton's model, calculate shock-induced internal-mode transition rates for nitromethane, and attempt to relate our results to critical-shock initiation data for nitromethane.

II. MODEL OF SHOCKED SOLID

When a shock wave travels through a solid, lattice normal modes are excited to higher levels, that is, acoustic photons are created. The shock also compresses the solid, causing the frequency of the acoustic modes to increase. The central issue is to calculate the rate at which acoustic-mode energy is transferred to molecular internal modes. For this purpose, it is assumed that the distribution of acoustic-mode energy relaxes to a thermal distribution in a time which is short compared to the time required to create a significant number of optical (internal-mode) phonons. Thus one immediate effect of the shock is to raise the temperature of the acoustic modes while leaving the internal modes "cold." The nonradiative transition rates between internal-mode levels then give an estimate of the rate at which the internal modes relax to the new, higher temperature. Since the transition rates depend on the acoustic-mode frequencies, it will be necessary to determine the change in frequency produced by the shock. The change in average acoustic-mode frequency can be deduced approximately from the compression by integrating the Grüneisen parameter along the shock Hugoniot curve. Hence, in this model, the shock is

characterized by two quantities: the compression and the acoustic-mode temperature produced by the shock.

The assumption of rapid thermalization of the acoustic modes is reasonable since internal-mode frequencies are generally much higher than lattice-mode frequencies and this mismatch should greatly reduce the rate of energy transfer between lattice and internal modes compared to the rate among lattice modes.

The work of Van Vleck shows that the acoustic modes should thermalize on a picosecond time scale.[3] Van Vleck computes the rate of energy transfer between lattice oscillators due to anharmonic perturbations when different portions of the frequency spectrum are not in thermal equilibrium. His result for the transition rate from level n to level $n-1$ for a particular lattice oscillator when the main body of lattice oscillations is at a temperature T is

$$W_{n \to n-1} \sim nD(T/T_D)^2 v_D^5 , \qquad (1)$$

where v_D is the Debye frequency, T_D is the Debye temperature, and D is a constant characteristic of the particular solid. The value of D is about 10^{-51} sec^4 for typical solids. Equation (1) is valid for $T > T_D$. For $n=1$, $T=300$ K, and $v_D \sim 3 \times 10^{12}$ Hz, Eq. (1) gives transition lifetimes of the order of 10^{-12} sec.

Van Vleck used first-order perturbation theory to calculate the transition rate. While this may be satisfactory in the case of lattice relaxation, it will prove unsatisfactory in most cases for lattice internal-mode relaxation since internal-mode frequencies may be an order of magnitude greater than lattice mode frequencies. For this reason, a Born-Oppenheimer approximation analogous to the adiabatic approximation which has been used in treating the coupling of localized electronic states to lattice vibrations[4] is used here. In this formalism, the lattice modes are considered the slow subsystem and the internal modes are considered the fast subsystem. The approximation improves as the disparity between internal and lattice frequencies increases. Lin describes a similar formalism.[5]

III. CALCULATION OF NONRADIATIVE TRANSITION RATES

A. Nonadiabatic operator

In the Born-Oppenheimer approximation the total Hamiltonian H of the system is separated into two parts, the adiabatic part $\mathscr{H}$ and the nonadiabatic part $\mathscr{L}$. The Born-Oppenheimer basis states are eigenfunctions of $\mathscr{H}$. The nonadiabatic part $\mathscr{L}$ can be considered as an interaction which induces nonradiative transitions between stationary Born-Oppenheimer states.

Let n_κ be the acoustic-mode quantum number for a mode of frequency ω_κ. Let i be an internal-mode quantum number for an initial internal-mode state and let f be the quantum number for the final internal-mode state. Let n denote the set of initial acoustic-mode quantum numbers $\{n_\kappa\}$ and let m denote the set of final acoustic-mode quantum numbers $\{m_\kappa\}$. Then the transition rate from the initial to final state produced by the nonadiabatic interaction is obtained from first-order time-dependent perturbation theory:

$$W(i,n \to f,m) = \frac{2\pi}{\hbar} |\langle f,m | \mathscr{L} | i,n \rangle|^2 \delta(E_{fm} - E_{in}) . \qquad (2)$$

We are interested in the total transition rate assuming a thermalized distribution of acoustic-mode levels, so we must sum Eq. (2) over final acoustic states m and average it over initial acoustic states n. The result is

$$W(i \to f) = \frac{2\pi}{\hbar} \sum_{m,n} P_n |\langle f,m | \mathscr{L} | i,n \rangle|^2 \delta(E_{fm} - E_{in}) , \qquad (3)$$

where P_n is the probability that an acoustic state with quantum numbers $\{n_\kappa\}$ is realized. For a thermalized distribution, this is a Boltzmann probability distribution:

$$P_n = Q^{-1} e^{-\beta E_n} , \qquad (4a)$$

$$Q = \sum_n e^{-\beta E_n} , \qquad (4b)$$

$$\beta = 1/kT , \qquad (4c)$$

$$E_n = \sum_\kappa (n_\kappa + \tfrac{1}{2}) \hbar \omega_\kappa . \qquad (4d)$$

When the slow subsystem is a collection of harmonic oscillators the matrix elements of the nonadiabatic operator are[6]

$$\langle fm | \mathscr{L} | in \rangle = -\sum_\kappa \hbar \omega_\kappa \left[\left\langle \psi_f \phi_{fm} \left| \frac{\partial \psi_i}{\partial q_k} \frac{\partial \phi_{in}}{\partial q_\kappa} \right. \right\rangle \right.$$
$$\left. + \frac{1}{2} \left\langle \psi_f \phi_{fm} \left| \frac{\partial^2 \psi_i}{\partial q_\kappa^2} \phi_{in} \right. \right\rangle \right] , \qquad (5)$$

where ψ_i and ψ_f are internal-mode wave functions, ϕ_{in} and ϕ_{fm} are acoustic-mode wave functions, and q_κ are dimensionless acoustic-mode normal coordinates such that the kinetic energy operator has the form

$$T = -\tfrac{1}{2} \sum_\kappa \hbar \omega_\kappa \frac{\partial^2}{\partial q_\kappa^2} . \qquad (6)$$

If we assume that the reduced matrix elements

$$\mathscr{L}_{\kappa fi} = -\hbar \omega_\kappa \left\langle \psi_f \left| \frac{\partial \psi_i}{\partial q_\kappa} \right. \right\rangle , \qquad (7a)$$

$$\mathscr{M}_{\kappa fi} = -\tfrac{1}{2} \hbar \omega_\kappa \left\langle \psi_f \left| \frac{\partial^2 \psi_i}{\partial q_\kappa^2} \right. \right\rangle \qquad (7b)$$

do not depend on the acoustic coordinates q_κ (our "Condon approximation"), then we may write

$$\langle fm | \mathscr{L} | in \rangle = \sum_\kappa \left[\mathscr{L}_{\kappa fi} \left\langle \phi_{fm} \left| \frac{\partial \phi_{in}}{\partial q_\kappa} \right. \right\rangle \right.$$
$$\left. + \mathscr{M}_{\kappa fi} \langle \phi_{fm} | \phi_{in} \rangle \right] . \qquad (8)$$

While the Condon approximation is often a good one in dealing with electronic states, its validity is more ques-

tionable in this case. However, the simplification it produces is considerable. Similarly, it is often assumed that the $\mathcal{M}_{\kappa fi}$ term in Eq. (8) can be neglected compared to the $\mathcal{L}_{\kappa fi}$ term since the $\mathcal{M}_{\kappa fi}$ term contains the second derivative of the wave function with respect to the slow system coordinates. Because of the questionable validity of this assumption and because dropping the term leads to no appreciable simplification, we retain it.

B. Molecular lattice Hamiltonian

We write the Hamiltonian of a molecular lattice in the following form:

$$H = \sum_{n=1}^{3rN} \tfrac{1}{2} M_n \dot{u}_n^2 + V(u_1, \ldots, u_{3rN}) , \qquad (9)$$

where u_n is the nth Cartesian coordinate displacement from equilibrium, N is the total number of molecules, r is the number of atoms per molecule, and M_n is the mass of the atom associated with the nth coordinate. The potential energy V is a function of all the displacements. If we develop V in a power series we obtain

$$V = \sum_{m,n} V_{mn}^{(2)} u_m u_n + \sum_{l,m,n} V_{lmn}^{(3)} u_l u_m u_n + \cdots . \qquad (10)$$

There is no linear term in Eq. (10) since the u_n are displacements from equilibrium. Concentrating on the quadratic term in Eq. (10), we may find a transformation to real, dimensionless normal coordinates in the form

$$u_n = \sum_{j=1}^{3rN} A_{nj} \left[\frac{\hbar}{M_n \omega_j} \right]^{1/2} q_j , \qquad (11)$$

where A_{nj} is a real, orthogonal matrix. In the new coordinates, the Hamiltonian operator becomes

$$H = \sum_j \tfrac{1}{2} \hbar \omega_j \left[q_j^2 - \frac{\partial^2}{\partial q_j^2} \right] + \sum_{i,j,k} A_{ijk} q_i q_j q_k + \cdots , \qquad (12)$$

where

$$A_{ijk} = \sum_{l,m,n} A_{li} A_{mj} A_{nk} V_{lmn}^{(3)} \left[\frac{\hbar^3}{M_l M_m M_n \omega_i \omega_j \omega_k} \right]^{1/2} . \qquad (13)$$

Up to this point, we have made no distinction between lattice and internal modes. Now, following Toton,[2] we isolate one internal mode whose coordinate we designate q_0. Greek subscripts will designate acoustic-mode coordinates. Then the Hamiltonian may be written in the following form:

$$H = \tfrac{1}{2} \hbar \omega_0 \left[q_0^2 - \frac{\partial^2}{\partial q_0^2} \right] + \sum_\kappa \tfrac{1}{2} \hbar \omega_\kappa \left[q_\kappa^2 - \frac{\partial^2}{\partial q_\kappa^2} \right]$$
$$+ q_0 \sum_{\kappa,\lambda} B_{\kappa\lambda} q_\kappa q_\lambda + q_0^2 \sum_\kappa C_\kappa q_\kappa + \cdots . \qquad (14)$$

Since we are interested in the interaction between the internal mode q_0 and the acoustic modes q_κ, we have ig-

nored terms which involve interactions with internal modes other than q_0 and anharmonic terms which involve internal modes alone or acoustic modes alone.

C. Born-Oppenheimer separation

Following the Born-Oppenheimer prescription, we separate the Hamiltonian, Eq. (14), into the fast part

$$H_0 = \tfrac{1}{2} \hbar \omega_0 \left[-\frac{\partial^2}{\partial q_0^2} + (1+2C) q_0^2 + 2B q_0 + 2A \right] , \qquad (15)$$

where

$$\hbar \omega_0 A = \sum_\kappa \tfrac{1}{2} \hbar \omega_\kappa q_\kappa^2 ,$$

$$\hbar \omega_0 B = \sum_{\kappa,\lambda} B_{\kappa\lambda} q_\kappa q_\lambda ,$$

$$\hbar \omega_0 C = \sum_\kappa C_\kappa q_\kappa ,$$

and the slow part

$$H_1 = -\sum_\kappa \tfrac{1}{2} \hbar \omega_\kappa \frac{\partial^2}{\partial q_\kappa^2} . \qquad (16)$$

The Born-Oppenheimer basis functions, therefore, are products

$$\Psi(q_0, q_\kappa) = \psi(q_0, q_\kappa) \phi(q_\kappa) , \qquad (17)$$

where the first factor is a solution of the fast part

$$H_0 \psi_s = \epsilon_s(q_\kappa) \psi_s , \qquad (18)$$

and the second factor is a solution of

$$\left[-\sum_\kappa \tfrac{1}{2} \hbar \omega_\kappa \frac{\partial^2}{\partial q_\kappa^2} + \epsilon_s(q_\kappa) \right] \phi_{sn} = E_{sn} \phi_{sn} . \qquad (19)$$

The internal-mode quantum number is s and the collection of acoustic-mode quantum numbers is represented by n.

D. Internal-mode (fast subsystem) solution

Equation (18) is a harmonic-oscillator equation which we can reduce to standard form by making the change of variable

$$Z = \rho(q_0 - \bar{q}_0) , \qquad (20)$$

where

$$\rho^4 = 1 + 2C , \qquad (21)$$

$$\bar{q}_0 = -\rho^{-4} B . \qquad (22)$$

Then Eq. (18) becomes

$$\left[-\tfrac{1}{2} \hbar \omega_0 \rho^2 \left[\frac{\partial^2}{\partial Z^2} - Z^2 \right] + \tfrac{1}{2} \hbar \omega_0 (2A - \rho^{-4} B^2) \right] \psi_s$$
$$= \epsilon_s \psi_s , \qquad (23)$$

with energy eigenvalues

$$\epsilon_s(q_\kappa) = (s + \tfrac{1}{2})\hbar\omega_0 \rho^2$$

$$+ (A - \tfrac{1}{2}\rho^{-4}B^2)\hbar\omega_0, \quad s = 0,1,2,\dots . \quad (24)$$

The wave functions are

$$\psi_s(q_0, q_\kappa) = \sqrt{\rho}\,\psi_s^{(HO)}(Z) , \quad (25)$$

where $\psi_s^{(HO)}(Z)$ is a normalized harmonic-oscillator eigenfunction. The factor $\sqrt{\rho}$ normalizes the wave function as a function of q_0. Both the energy eigenvalues and the wave functions depend parametrically on the acoustic coordinates q_κ through the quantities A, B, and ρ.

E. Equilibrium acoustic normal coordinates

The equilibrium acoustic normal coordinates are determined by the energy eigenvalues, Eq. (24), which act as effective potentials for the acoustic-wave equation. The equilibrium coordinates are derived in Appendix A and the result [Eq. (A3)] is

$$q_{\kappa s} \simeq -(s + \tfrac{1}{2})\frac{C_\kappa}{\hbar\omega_\kappa} , \quad (26)$$

where $q_{\kappa s}$ is the equilibrium value of coordinate q_κ when the internal mode is in state s.

F. Nonadiabatic operator matrix elements

We may substitute the wave functions, Eq. (25), into Eqs. (7a) and (7b) to obtain the nonadiabatic-operator-reduced matrix elements $\mathscr{L}_{\kappa fi}$ and $\mathscr{M}_{\kappa fi}$. The calculation is outlined in Appendix B and the results are given in Eqs. (B6) and (B7). The matrix elements are functions of the acoustic coordinates, but, in the spirit of the Condon approximation, we will assume that they are constants with values obtained by substituting the equilibrium values of the acoustic coordinates for the internal mode in the initial state i. In addition, we assume that the third-order anharmonic corrections to the Hamiltonian, Eq. (14), are small so that the quantities $B, C \ll 1$ and $\rho \approx 1$.

The results of Appendix B indicate that the nonradiative transition rates are nonzero only for nearest-neighbor $(i \rightarrow i \pm 1)$ and next-nearest-neighbor $(i \rightarrow i \pm 2)$ transitions. Of these, the nearest-neighbor transition rates typically will be larger by many orders of magnitude. Thus from Eqs. (B6) and (B7) we obtain

$$\mathscr{L}_{\kappa,i+1,i} = \frac{\omega_\kappa}{\omega_0}[2(i+1)]^{1/2}$$

$$\times \left[\sum_\lambda B_{\kappa\lambda} q_{\lambda i} - \frac{C_\kappa}{\hbar\omega_0} \sum_{\kappa,\lambda} B_{\kappa\lambda} q_{\kappa i} q_{\lambda i} \right] , \quad (27)$$

$$\mathscr{M}_{\kappa,i+1,i} = \frac{\omega_\kappa}{\omega_0}[2(i+1)]^{1/2} B_{\kappa\kappa} . \quad (28)$$

G. Estimating normal-mode anharmonic coupling coefficients

Comparing Eqs. (13) and (14), we can obtain expressions for C_κ and $B_{\kappa\lambda}$ in terms of the third-order coeffi-

cients of the power-series development of the potential energy of the crystal. In particular, we write C_κ and $B_{\kappa\lambda}$ in the following suggestive forms:

$$C_\kappa = \frac{1}{\sqrt{N}} \frac{V_{3\kappa}}{M^{3/2}} \frac{\hbar^{3/2}}{\omega_0\sqrt{\omega_\kappa}} , \quad (29)$$

where

$$\frac{V_{3\kappa}}{\sqrt{N}M^{3/2}} = \sum_{l,m,n} \frac{A_{l0}A_{m0}A_{n\kappa}}{(M_l M_m M_n)^{1/2}} V_{lmn}^{(3)} , \quad (30)$$

$$B_{\kappa\lambda} = \frac{1}{\sqrt{N}} \frac{V_{3\kappa\lambda}}{M^{3/2}} \frac{\hbar^{3/2}}{(\omega_0\omega_\kappa\omega_\lambda)^{1/2}} , \quad (31)$$

$$\frac{V_{3\kappa\lambda}}{\sqrt{N}M^{3/2}} = \sum_{l,m,n} \frac{A_{l0}A_{m\kappa}A_{n\lambda}}{(M_l M_m M_n)^{1/2}} V_{lmn}^{(3)} . \quad (32)$$

In Eqs. (30) and (32), M is the mass of a molecule and N is the number of molecules. Since binding forces are not long range, the coefficients $V_{lmn}^{(3)}$ are significant only when l, m, n are nearly equal. Therefore, the triple sum has effectively the order of N terms. The orthogonal transformation coefficients A_{lj} are typically sinusoidal and proportional to $N^{-1/2}$. Therefore, C_κ is proportional to $NN^{-3/2} = N^{-1/2}$. It is clear that the energy eigenvalues in Eq. (24) should be essentially independent of the size of the system and so the quantity B appearing in Eq. (24) and defined after Eq. (15) should be essentially independent of N when B is evaluated for q_κ equal to the equilibrium values $q_{\kappa s}$. For this to be true, we require $B_{\kappa\lambda}$ to be proportional to N^{-1}. Then Eqs. (30) and (32) define average third-order coefficients $V_{3\kappa}$ and $V_{3\kappa\lambda}$.

Calculations for a linear diatomic chain indicate that, for a rough approximation, we may set $V_{3\kappa\lambda} \sim f'''(r_e)$ where $f(r)$ is a pair potential describing the intermolecular force and r_e is the equilibrium molecular separation.

H. Integral expression for the transition rate

The sum appearing in Eq. (3) can be converted to an integral by several methods summarized by Perlin in his review article.[4] One convenient method involves the use of the integral representation of the δ function.[7] The resulting transition rate is

$$W(i \rightarrow f) = \frac{1}{\hbar^2} \int_{-\infty}^{\infty} F_{fi}(t)\exp\left[i\omega_{fi}t \right.$$

$$\left. + \sum_\kappa F_\kappa(t)\Delta_{\kappa fi}^2 - S \right] dt , \quad (33a)$$

where

$$F_{fi}(t) = \sum_\kappa |\mathscr{L}_{\kappa fi}|^2 F_\kappa(t)$$

$$+ \sum_\kappa \mathscr{L}_{\kappa fi}\Delta_{\kappa fi}E_\kappa(t) \sum_\lambda \mathscr{L}_{\lambda fi}^*\Delta_{\lambda fi}E_\lambda(t)$$

$$+ \sum_{\kappa,\lambda} (\mathscr{M}_{\kappa fi}^*\mathscr{L}_{\lambda fi} + \mathscr{M}_{\kappa fi}\mathscr{L}_{\lambda fi}^*)\Delta_{\lambda fi}E_\lambda(t)$$

$$+ \left| \sum_\kappa \mathscr{M}_{\kappa fi} \right|^2 , \quad (33b)$$

and where

$$F_\kappa(t) = \frac{\cosh(i\omega_\kappa t + \frac{1}{2}\beta\hbar\omega_\kappa)}{2\sinh(\frac{1}{2}\beta\hbar\omega_\kappa)} ,$$ (33c)

$$E_\kappa(t) = F_\kappa(t) - \frac{1}{2}\coth(\frac{1}{2}\hbar\omega_\kappa) ,$$ (33d)

$$S = \sum_\kappa \frac{1}{2}\coth(\frac{1}{2}\beta\hbar\omega_\kappa)\Delta^2_{\kappa fi} ,$$ (33e)

$$\Delta_{\kappa fi} = q_{\kappa f} - q_{\kappa i} .$$ (33f)

In Eq. (33f), $q_{\kappa f}$ and $q_{\kappa i}$ are the equilibrium values of the dimensionless acoustic normal coordinate q_κ when the internal mode is in states f and i, respectively.

I. Approximate evaluation of the transition-rate integral

An approximate evaluation of the integral in Eq. (33a) may be obtained by the method of steepest descents as described by Perlin.[4] The result is still somewhat unwieldy so we make the further approximation that the sums over the acoustic modes can be replaced by sums in which the frequencies ω_κ are replaced by some average frequency ω_D. For convenience, we will refer to ω_D as the Debye frequency since there is some evidence that the average frequency determined from the lattice infrared absorption spectrum correlates well with the Debye frequency determined by other methods, for example, from specific-heat data.[8]

In Eq. (33a), if we make the change of variable $z = it$, then the transition-rate expression becomes

$$W(i \to f) = \frac{1}{i\hbar^2} \int_{-i\infty}^{i\infty} F_{fi}(-iz)e^{g(z)}dz ,$$ (34)

where

$$g(z) = \omega_{fi}z + \sum_\kappa \frac{\cosh(\omega_\kappa z + \frac{1}{2}\beta\hbar\omega_\kappa)}{2\sinh(\frac{1}{2}\beta\hbar\omega_\kappa)}\Delta^2_{\kappa fi} - S .$$ (35)

At a saddle point z_0, $g'(z_0) = 0$. It is easily verified that $g'(z)$ has many complex roots but precisely one real root. Deforming the contour of integration to pass through the real root z_0, we obtain the approximate transition rate

$$W(i \to f) = \frac{1}{\hbar^2}\left[\frac{2\pi}{g''(z_0)}\right]^{1/2} F_{fi}(-iz_0)\exp[g(z_0)] .$$ (36)

If we replace the acoustic frequencies ω_κ by the single average frequency ω_D, the equation $g'(z_0) = 0$ becomes

$$p = x\sinh(\omega_D z_0 + \frac{1}{2}\beta\hbar\omega_D) ,$$ (37)

where

$$p \equiv -\frac{\omega_{fi}}{\omega_D}$$ (38)

and

$$x = \frac{S_0}{\sinh(\frac{1}{2}\beta\hbar\omega_D)} .$$ (39)

The dimensionless quantity S_0, introduced by Huang and Rhys,[9] is a measure of the strength of the anharmonic coupling between a given internal mode and the acoustic modes. It is a function of the difference in acoustic coordinate equilibrium values in the internal-mode state i versus internal-mode state f:

$$S_0 = \frac{1}{2}\sum_\kappa \Delta^2_{\kappa fi} .$$ (40)

Using Eqs. (29) and (31) as a guide, we can approximate the coefficients C_κ and $B_{\kappa\lambda}$ as follows:

$$C_\kappa = \frac{f_1\alpha}{\sqrt{N}\sqrt{\omega_D}\omega_0}\left[\frac{\hbar}{M}\right]^{3/2} ,$$ (41)

$$B_{\kappa\lambda} = \frac{f_2\alpha}{N\omega_D\sqrt{\omega_0}}\left[\frac{\hbar}{M}\right]^{3/2} .$$ (42)

The quantity α denotes $f'''(r_e)/2$. The quantities f_1 and f_2 are dimensionless numbers which we will set to $1/\sqrt{2}$ and 2, respectively. By combining these expressions with the expressions for the nonadiabatic operator matrix elements [Eqs. (27) and (28)], the Huang-Rhys factor [Eq. (40)], the equilibrium acoustic coordinates [Eq. (26)], and Eq. (33b) we obtain (see Appendix C) the following expression for the nonradiative transition rate:

$$W(i \to f) = \sqrt{2\pi}\omega_D \frac{1}{\sqrt{P}}\exp[g(z_0)]\frac{F_{fi}}{(\hbar\omega_D)^2} ,$$ (43)

where

$$\exp[g(z_0)] = \left[\frac{x}{|p| + P}\right]^{|p|}\exp\left[\frac{\hbar\omega_D}{2kT}p + P - S\right] ,$$ (44)

$$\frac{F_{fi}}{(\hbar\omega_D)^2} = 8\frac{S_0}{|p|}[(i+1)\delta_{f,i+1} + i\delta_{f,i-1}]$$

$$\times[(2i+1)^2(P-S)^2 + 4(2i+1)(P-S)$$

$$+ (2i+1)^2 P + 4] ,$$ (45)

$$P = (p^2 + x^2)^{1/2} ,$$ (46)

$$S = S_0\coth(\frac{1}{2}\beta\hbar\omega_D) .$$ (47)

For up transitions, the final state $f = i + 1$ so that $\omega_{fi} = \omega_0$ where ω_0 is the internal-mode vibrational frequency. For down transitions, $f = i - 1$ so that $\omega_{fi} = -\omega_0$. T is the temperature of the thermalized acoustic modes.

IV. RELATION OF HUANG-RHYS FACTOR TO INFRARED SPECTRUM

A. Huang-Rhys factor related to moments of spectral distribution

It was pointed out by Lax[10] that the Huang-Rhys factor S_0 is directly related to the moments of distribution of the radiative absorption or emission spectrum. From the first moment we obtain

$$\Delta\Omega = 2S_0\omega_D ,$$ (48)

where $\Delta\Omega$ is the difference between the means of the emission and absorption bands. Perlin[4] calls $\Delta\Omega$ the Stokes parameter. The second, third, and fourth moments give

$$\sigma^2 \equiv \langle (\omega - \overline{\omega})^2 \rangle = \omega_D^2 S_0 \coth(\tfrac{1}{2}\beta\hbar\omega_D) , \qquad (49)$$

$$\gamma_3 \equiv \frac{\langle (\omega - \overline{\omega})^3 \rangle}{\sigma^3} = [(S_0)^{1/2}\coth(\tfrac{1}{2}\beta\hbar\omega_D)]^{-1} , \qquad (50)$$

$$\gamma_4 \equiv \frac{\langle (\omega - \overline{\omega})^4 \rangle}{\sigma^4} - 3 = [S_0\coth(\tfrac{1}{2}\beta\hbar\omega_D)]^{-1} . \qquad (51)$$

The skewness γ_3 and kurtosis γ_4 are measures of the deviation from a Gaussian distribution. If the distribution were Gaussian, it would be possible to determine S_0 by measuring the full width at half maximum, $\Delta\omega$, since, in this case,

$$\Delta\omega = 2(2\ln 2)^{1/2}\sigma , \qquad (52)$$

B. Spectral band shape not Gaussian

Unfortunately, we see by examining the expressions for skewness and kurtosis [Eqs. (50) and (51)] that the deviation from a Gaussian distribution is considerable if $S_0 \ll 1$ which is the case for internal-mode vibrations. Typical internal-mode frequencies lie in the range 500–2500 cm^{-1} (10^{14}–5×10^{14} sec^{-1}) with typical infrared absorption bandwidths of 10–50 cm^{-1}. Typical Debye frequencies are around 100 cm^{-1} (2×10^{13} sec^{-1} or 150 K). Thus $\Delta\omega/\omega_D \sim 0.2$ which implies, from Eq. (49), that $S \sim \frac{1}{200}$ and, therefore, if $T > 75$ K, that $S_0 < \frac{1}{200}$. This is in sharp contrast to the situation for electronic transitions in F centers[9] where $\Delta\omega \sim 2000$–5000 cm^{-1} so that $S_0 \sim 20$.

C. How to determine Huang-Rhys factor

It is practically impossible to determine experimentally the moments of a typical infrared spectra band due to the presence of noise. Besides the mean frequency, the width at half maximum is about the only parameter which can be measured with any degree of accuracy. However, it is possible to relate the bandwidth and the Stokes parameter since the relation to the higher moments is also known. A band-shape function with arbitrary third and fourth moments as parameters is chosen and the moments are constrained to satisfy Eqs. (49)–(51). Then S_0 can be determined from the bandwidth by finding the root of a transcendental equation. In particular, the function

$$I(x) = \phi(x) - \frac{\gamma_3}{3!}\phi^{(3)}(x) + \frac{\gamma_4}{4!}\phi^{(4)}(x) , \qquad (53)$$

where

$$\phi(x) = \exp(-\tfrac{1}{2}x^2)\sqrt{2\pi} \qquad (54)$$

is a normalized distribution with zero mean, unit standard deviation, skewness γ_3, and excess γ_4. Now let $x = (\omega - \overline{\omega})/\sigma$ and substitute for σ, γ_3, and γ_4 from Eqs. (49)–(51). If we then set $I(x) = I(0)/2$, we obtain an equation which can be solved numerically for S_0, given

$(\omega - \overline{\omega})/\omega_D$. Another distribution, quoted by Lax[10] as being due to Edgeworth, includes a sixth derivative:

$$I(x) = \phi(x) - \frac{\gamma_3}{3!}\phi^{(3)}(x) + \frac{\gamma_3}{4!}\phi^{(4)}(x) + \frac{10\gamma_3^2}{6!}\phi^{(6)}(x) . \qquad (55)$$

The distribution, Eq. (55), does not provide a significantly better match for the higher moments.

D. Saddle-point approximation not good for radiative transitions

By using the method of moments we have not found it necessary to actually evaluate the integral for the spectral band shape. This is fortunate since the saddle-point approximation which we used for the nonradiative transition rates is not a good one for the radiative rates. This point is discussed in Appendix D.

V. APPLICATION TO NITROMETHANE

A. Liquid versus crystalline nitromethane

In this section we apply the results of the preceding sections to the extensively studied and relatively simple condensed explosive material, nitromethane. One caveat is necessary, however. Under normal conditions, nitromethane is a liquid and even under the extreme conditions characteristic of detonations it most likely retains the structure of a liquid.[11] The previous results apply, strictly speaking, to a material which has long-range periodic structure. It is not clear what the absence of such a structure would have on the predicted transition rates. In order to make a direct comparison with the results to be presented it will be necessary to perform shock experiments on solid nitromethane.

B. Parameters to be determined

In order to apply the transition rate formula, Eq. (43), we need four parameters for a material. Two are characteristic of the state of the shocked material: the Debye frequency ω_D and the temperature T. Two are characteristic of the internal mode whose transition rate is to be determined: the vibration frequency ω_0 and the Huang-Rhys parameter S_0.

The Debye frequency is a function of compression which, in turn, is directly related to the shock pressure via the hugoniot relation. The internal-mode vibrational frequencies are only slightly affected by compression[12] so that we can safely assume them to be constant.

C. Huang-Rhys factors for nitromethane

The variation of the Huang-Rhys factor S_0 with compression is not known. However, S_0 depends both on the acoustic frequencies and the displacement of acoustic coordinate equilibrium positions. The way in which the displacements change depends in detail on the anharmonic part of the intermolecular forces. If we examine the ap-

TABLE I. Huang-Rhys parameters for some optically active internal modes of nitromethane (CH_3NO_2). Bandwidths were measured from infrared absorption spectra obtained in a diamond-anvil cell at room temperature (295 K) and pressures of the order of 5—18 kbar. Spectra obtained by J. W. Brasch, Jr., Naval Surface Weapons Center.

Mode	ω_0 (cm^{-1})	$\Delta\omega$ (cm^{-1})	S_0 [Eq. (53)]	S_0 [Eq. (55)]
CH_3 rocking parallel to NO_2 plane	1104	29±6	1.47×10^{-2}	1.39×10^{-2}
C—N stretch	923	6.5±1.1	1.01×10^{-3}	9.6×10^{-4}
NO_2 symmetric bending	663	19±2.3	7.3×10^{-3}	6.9×10^{-3}
NO_2 rocking perpendicular to NO_2 plane	609	8.2±1.1	1.58×10^{-3}	1.50×10^{-3}
NO_2 rocking parallel to NO_2 plane	485	7.6±1.5	1.37×10^{-3}	1.30×10^{-3}

proximate expression for S_0 given in Appendix C [Eq. (C2)] we see that $S_0 \sim \alpha^2/\omega_D^3$ where α is the third-order coefficient in the series expansion of the interparticle potentials. A straightforward calculation would show a substantially different variation of S_0 with compression for (for example) a Morse potential as contrasted with a power law (e.g., 6-12) potential. Measurements indicate that bandwidths of infrared absorption bands increase slightly with compression leading to the conclusion that S_0 has only a weak dependence on compression (at least for nitromethane). In the absence of more definitive data at the present time we will assume that S_0 is constant. Table I lists values for several optically active internal modes of nitromethane. The values are calculated from the bandwidths using the method described previously. Two values of S_0 are given corresponding to the two slightly different representations of the band shape, Eqs. (53) and (55). We should note here that the optically active modes are a subset of the tiny fraction of modes which have zero wave number out of the total of approximately Avogadro's number of internal modes.

The data from which S_0 is calculated were obtained in a diamond anvil cell at room temperature (295 K) and relatively low pressures (5—18 kbar) by Brasch of the Naval Surface Weapons Center. The nitromethane is in a solid polycrystalline form under these conditions.

The values calculated for S_0 are for a Debye frequency of 2×10^{13} rad/sec (106.2 cm^{-1} or 152.7 K). It was determined that this is a reasonable value for the Debye frequency at standard temperature and pressure by taking the centroid of the low-frequency part of the infrared absorption spectrum of nitromethane.

D. Transition rates versus Debye frequency and temperature

In Fig. 1 are the transition rates given by Eq. (43) for the internal modes listed in Table I using the values of S_0 given in the next to last column of the table. The transition rate is plotted as a function of ω_D for 300 K (solid curves) and for 2100 K (dashed curves). The most noticeable feature of the curves is the large variation in transition rates with relatively small changes in ω_0, ω_D, and T. The C—N stretching mode, with a frequency of 1.74×10^{14} sec^{-1} has a ground to first excited state transition rate of about 10^{-17} sec^{-1} at a temperature of 300 K

and ω_D of 2×10^{13} sec^{-1} (this point is beyond the scale of the graph). On the other hand, the NO_2 symmetric bending mode with about two-thirds the C—N stretching frequency, 3 times the C—N stretch bandwidth, at 7 times higher temperature and 2 times higher Debye frequency has a transition rate of 10^9 sec^{-1}, 26 orders of magnitude greater.

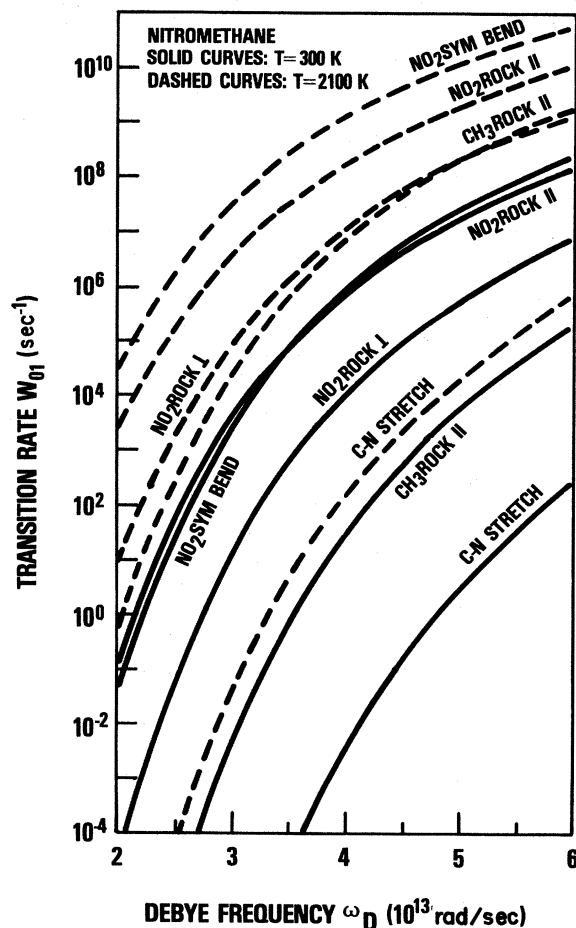FIG. 1. Transition rates vs Debye frequency for several internal modes of nitromethane. Solid curves for $T=300$ K, dashed curves for $T=2100$ K.

One conclusion to be drawn from Fig. 1 is that energy is initially transferred most rapidly into the lowest-frequency internal mode, NO_2 rocking parallel to the NO_2 plane at 485 cm^{-1}. This is not to say that there are not other internal modes into which energy is transferred more rapidly since we can survey here only the optically active modes. There are many internal modes with nonzero wave number which are not optically active and about which we presently have no transition rate information. We are discounting the NO_2 symmetric bending mode since the calculated large transition rate is due to its large apparent bandwidth and the band may actually be the superposition of two individual bands.

Another conclusion to be drawn from Fig. 1 is that small increases in temperature and compression (compression increases the Debye frequency) will lead to large increases in the rate of energy transfer. We also note that the relative importance of the internal modes in energy relaxation can change with changes in temperature and compression. For example, at 300 K, the CH_3 rocking parallel to the NO_2 plane (CH_3 rock $||$) has a significantly lower excitation rate than the NO_2 rocking perpendicular to the NO_2 plane (NO_2 rock $\perp$), while at 2100 K the excitation rates are comparable, with the CH_3 rocking parallel mode rate exceeding that of the NO_2 rocking perpendicular mode rate at the higher values of ω_D.

Inserting numerical values in Eq. (43), we discover that W_{12} is typically 10 times greater than W_{01}, and W_{23} is typically 40 times greater. Thus the relaxation time for energy distribution among the low-lying internal levels is determined by the ground to first excited state transition rate, W_{01}. We cannot say anything about transitions between levels lying near the top of the potential well since our analysis assumes a harmonic internal-mode potential. At this point we can only say that, if the transitions between levels close to dissociation are also rapid, then the rate W_{01} would be the significant parameter determining the overall dissociation rate. We may expect energy to be redistributed between internal modes more rapidly than it would be transferred between acoustic and internal modes. Thus the overall internal-mode thermal relaxation time as well as the overall dissociation rate should be controlled by W_{01} for the fastest internal mode (which seems to be the NO_2 rocking parallel made in nitromethane).

E. Relation of Debye frequency to compression

The relation of Debye frequency to compression can be determined approximately by using the expression for the Grüneisen parameter which arises in the Debye model of a solid,

$$\gamma = -\frac{d\ln\omega_D}{d\ln v} \, , \tag{56}$$

where γ is the Grüneisen parameter and v is the specific volume.[13] Integrating Eq. (56) we obtain

$$\frac{\omega_D}{\omega_{D0}} = \exp\left[- \int_{\ln v_0}^{\ln v} \gamma d\ln v \right] . \tag{57}$$

Hardesty and Lysne[11] have calculated the thermodynamic properties of shocked nitromethane along hugoniots for initial pressure of 1 bar and initial temperatures of 244 298, and 373 K. If we numerically integrate their Grüneisen-parameter data according to Eq. (57), we obtain the results shown in the log-log plot of Fig. 2. It is assumed that $\omega_{D0} = 2 \times 10^{13}$ sec^{-1}. From Fig. 2 we see that above 5 kbar the curves are nearly linear indicating an approximate power-law relation. The dashed lines are isotherms showing the shock temperature on each hugoniot.

F. Transition rates along a hugoniot

Using the results shown in Fig. 2 we can plot the transition rates versus pressure along a hugoniot. This is done in Fig. 3 for the hugoniot with initial temperature 298 K. Figure 3 is a log-log plot showing very close to power-law curves above 5 kbar.

G. Pressure-time critical relation

If we disregard the NO_2 symmetric bending mode, the NO_2 rocking mode parallel to the NO_2 plane is the mode whose transition rate is the most important in energy transfer from the acoustic modes. If the transition rates calculated from Eq. (43) are approximately correct and if the transition rate for the NO_2 rocking parallel mode is the controlling factor in the overall dissociation chain, then the plot of transition rate versus shock pressure for
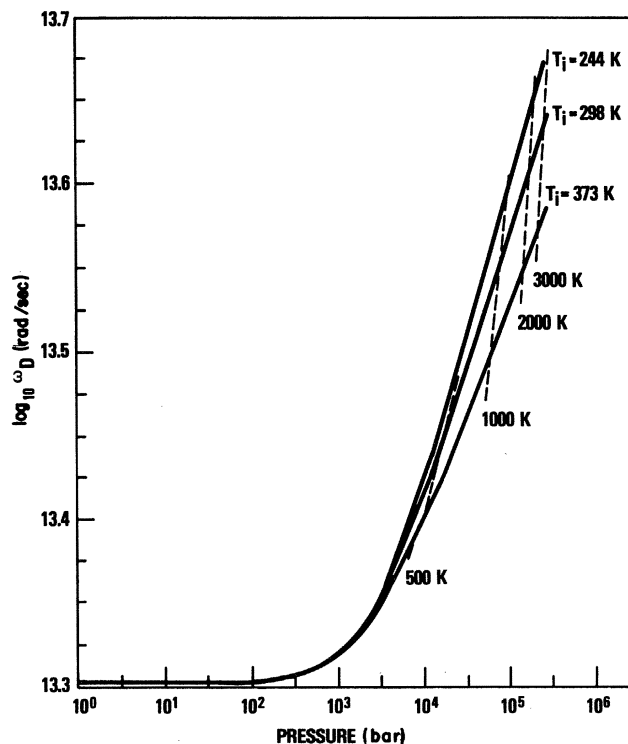

FIG. 2. Debye frequency of nitromethane as a function of pressure along three shock Hugoniots with initial temperatures of 244, 298, and 373 K.
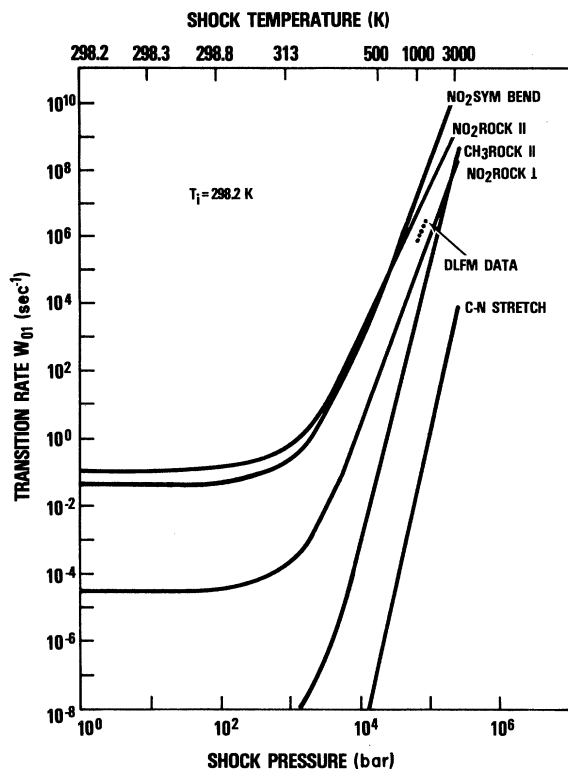
FIG. 3. Nonradiative (shock-induced) transition rates for several internal modes of nitromethane plotted as a function of shock pressure along the Hugoniot with initial temperature 298 K. The points marked DLFM are the critical-shock initiation data obtained by de Longueville, Fauquignon, and Moulard.

this mode provides a pressure-time criterion for initiation of reactions. Thus it is clear that a shock of a given pressure must be sustained for a time which is some multiple (of order unity) of W_{01}^{-1} in order for significant dissociation to occur.

H. Comparison with pressure-time critical initiation data

In this regard, de Longueville, Fauquignon, and Moulard (DLFM) reported critical initiation data in the pressure-time plane for several condensed explosives including nitromethane.[14] We have included that data shown as a short-dotted line segment labeled DLFM in Fig. 3. The inverse of DLFM's time is plotted on the ordinate, W_{01}. It is interesting, though possibly coincidental, that the DLFM data, over its limited range, show times that are approximately 6–7 times the NO_2 rocking parallel mode transition lifetimes at the corresponding pressures and the curve segments show roughly the same slope.

VI. CONCLUSION

We have presented a quantum-mechanical calculation of the transition rates for shock-induced transitions between the low-lying internal molecular normal modes in a molecular solid. We have assumed that the shock pro-

duces a distribution of acoustic phonons which become thermalized before any significant internal-mode phonons are created. This assumption seems to have been justified in the case of nitromethane in which the shortest internal-mode transition lifetimes are of the order of nanoseconds while lattice relaxation times determined from Van Vleck's calculation are of the order of picoseconds or less. In particular, at the von Neumann spike pressure in nitromethane (about 200 kbar), the NO_2 rocking (parallel to NO_2 plane) mode has an excitation time of about 4 nsec.

When we compared the excitation lifetimes with the pressure-time critical initiation data of DLFM, we found that the times were not inconsistent with the hypothesis that the overall dissociation rate limiting factor is the relaxation time (W_{01}^{-1}) for transferring energy from the acoustic modes to a limited number of internal molecular modes (NO_2 rocking parallel to the NO_2 plane in nitromethane).

We must reiterate, however, that the numbers we have obtained for nitromethane are subject to many uncertainties, among them, uncertainties in determining the Huang-Rhys factor S_0 for each mode and the uncertainty in a suitable choice of Debye frequency ω_D. Small changes in both of these quantities lead to large changes in the transition rates. Also, for the great majority of modes which are not optically active, it is not possible to determine S_0. Perhaps the results of neutron scattering experiments may give useful information on these modes. Other problems are the question of the validity of the Condon approximation [Eq. (8)], the determination of the anharmonic coupling coefficients [Eqs. (41) and (42)], the validity of isolating one internal mode, neglecting the interaction between internal modes, and the use of a single frequency ω_D to characterize the acoustic spectrum. Finally, the shock data available for nitromethane is for the liquid state whereas the calculations, strictly speaking, apply to the solid state. We hope that experimenters will be encouraged to undertake shock experiments on solid nitromethane in order to obtain both Hugoniot data and critical initiation data. In order to apply the results presented here to other solid explosives it is necessary that the explosive be homogeneous and have an internal-mode spectrum clearly distinguished and well separated from the lattice spectrum.

Note added. Our attention has recently been drawn to papers by Kono and Lin[15] in which the Born-Oppenheimer approximation has been used to separate high- and low-frequency vibrations in solids.

APPENDIX A: ACOUSTIC-MODE WAVE EQUATION APPROXIMATE SOLUTIONS

The internal-mode eigenvalues, Eq. (24), are the effective potentials which determine the acoustic-mode Born-

Oppenheimer wave functions via Eq. (19). To obtain an approximate solution, expand the eigenvalues ϵ_f in powers of q_κ up to quadratic terms. This is a good approximation if the anharmonic corrections to the total Hamiltonian are small so that $B, C \ll 1$. Then

$$\frac{\partial \epsilon_s}{\partial q_\kappa} \simeq (s + \tfrac{1}{2})C_\kappa + \hbar\omega_\kappa q_\kappa \tag{A1}$$

and

$$\frac{\partial^2 \epsilon_s}{\partial q_\kappa \partial q_\kappa} \simeq \hbar\omega_\kappa \delta_{\kappa\lambda} - (s + \tfrac{1}{2})\frac{C_\kappa C_\lambda}{\hbar\omega_0} \;. \tag{A2}$$

Thus the equilibrium acoustic coordinates are

$$q_{\kappa s} \simeq -(s + \tfrac{1}{2})\frac{C_\kappa}{\hbar\omega_\kappa} \tag{A3}$$

and the effective potential is

$$\epsilon_s \simeq \epsilon_s(q_{\kappa s}) + \sum_\kappa \tfrac{1}{2}\hbar\omega_\kappa (q_\kappa - q_{\kappa s})^2 \;. \tag{A4}$$

In Eq. (A4) we have ignored the off-diagonal quadratic terms since they are small under our previous assumptions. These terms lead to mixing of the acoustic coordinates and subsequent modifications of the acoustic frequencies. In terms of the variables $\tilde{q}_\kappa = q_\kappa - q_{\kappa s}$, the acoustic-wave equation, Eq. (19), becomes

$$\left[\sum_\kappa \tfrac{1}{2}\hbar\omega_\kappa \left(\tilde{q}_\kappa^2 - \frac{\partial^2}{\partial \tilde{q}_\kappa^2} \right) + J_s \right] \phi_{sn} = E_{sn}\phi_{sn} \;, \tag{A5}$$

where

$$J_s = (s + \tfrac{1}{2})\hbar\omega_0 - \sum_\kappa \tfrac{1}{2}\hbar\omega_\kappa q_{\kappa s}^2 \;. \tag{A6}$$

Thus the total-energy eigenvalues are

$$E_{sn} = J_s + \sum_\kappa (n_\kappa + \tfrac{1}{2})\hbar\omega_\kappa \;. \tag{A7}$$

APPENDIX B: EVALUATION OF $\mathscr{L}_{\kappa fi}$ AND $\mathscr{M}_{\kappa fi}$

Using the result in Eq. (25) we obtain

$$\left[\psi_f, \frac{\partial \psi_i}{\partial q_\kappa} \right] = \int \sqrt{\rho}\,\psi_f^{(HO)}(Z)\frac{\partial}{\partial q_\kappa}[\sqrt{\rho}\,\psi_i^{(HO)}(Z)]dq_0 \;, \tag{B1}$$

and, transforming the variable of integration from q_0 to Z, the result is

$$\left[\psi_f, \frac{\partial \psi_i}{\partial q_\kappa} \right] = \int \psi_f^{(HO)}(Z)\frac{d\psi_i^{(HO)}(Z)}{dZ}\frac{\partial Z}{\partial q_\kappa}dZ$$

$$+ \frac{\partial}{\partial q_\kappa}(\ln\sqrt{\rho})\delta_{fi} \;. \tag{B2}$$

Since $f \neq i$, the second term in Eq. (B2) is zero. Differentiating Eq. (20) we obtain

$$\hbar\omega_0 \frac{\partial Z}{\partial q_\kappa} = \tfrac{1}{2}\rho^{-4}C_\kappa Z + 2\rho^{-3}\sum_\lambda B_{\kappa\lambda}q_\lambda - 2\rho^{-7}BC_\kappa \;. \tag{B3}$$

Using Eqs. (B3), (B2), and (7a) we obtain

$$\mathscr{L}_{\kappa fi} = -\frac{\hbar\omega_\kappa}{\hbar\omega_0} \left[\tfrac{1}{2}\rho^{-4}C_\kappa \left\langle f \left| Z\frac{\partial}{\partial Z} \right| i \right\rangle \right.$$

$$+ 2 \left[\rho^{-3}\sum_\lambda B_{\kappa\lambda}q_\lambda - \rho^{-7}BC_\kappa \right]$$

$$\left. \times \left\langle f \left| \frac{\partial}{\partial Z} \right| i \right\rangle \right] \;, \tag{B4}$$

where $\langle f | Z(\partial/\partial Z) | i \rangle$ and $\langle f | (\partial/\partial Z) | i \rangle$ are the usual harmonic-oscillator matrix elements. These may be evaluated most conveniently by writing Z and $\partial/\partial Z$ in terms of the creation and annihilation operators, $a^\dagger$ and a, and then using the raising and lowering properties of these operators:

$$Z = \frac{1}{\sqrt{2}}(a + a^\dagger) \;, \tag{B5a}$$

$$\frac{\partial}{\partial Z} = \frac{1}{\sqrt{2}}(a - a^\dagger) \;, \tag{B5b}$$

$$a^\dagger | n \rangle = \sqrt{n+1} | n+1 \rangle \;, \tag{B5c}$$

$$a | n \rangle = \sqrt{n} | n-1 \rangle \;. \tag{B5d}$$

The end result is

$$\mathscr{L}_{\kappa fi} = -\frac{\hbar\omega_\kappa}{\hbar\omega_0} \left[\sqrt{2} \left[\rho^{-3}\sum_\lambda B_{\kappa\lambda}q_\lambda - \rho^{-7}BC_\kappa \right](\sqrt{i}\,\delta_{f,i-1} - \sqrt{i+1}\,\delta_{f,i+1}) \right.$$

$$\left. + \tfrac{1}{4}\rho^{-4}C_\kappa\{[i(i-1)]^{1/2}\delta_{f,i-2} - \delta_{fi} - [(i+1)(i+2)]^{1/2}\delta_{f,i+2}\} \right] \;. \tag{B6}$$

A similar, though lengthier, calculation yields $\mathscr{M}_{\kappa fi}$. Since the result has many terms, we give here only the lowest-order term involving powers and products of C_κ and $B_{\kappa\lambda}$:

$$\mathscr{M}_{\kappa fi} = -\sqrt{2}\hbar\omega_\kappa \frac{B_{\kappa\kappa}}{\hbar\omega_0}(\sqrt{i}\,\delta_{f,i-1} - \sqrt{i+1}\,\delta_{f,i+1}) \;. \tag{B7}$$

APPENDIX C: APPROXIMATE TRANSITION-RATE FORMULA

Substitute Eq. (26) into Eq. (33f) and substitute the result into Eq. (40) to obtain the Huang-Rhys factor for a transition from state i to state f:

$$S_0 = \frac{(f-i)^2}{2\hbar^2\omega_D^2}\sum_\kappa C_\kappa^2 . \tag{C1}$$

The sum contains N terms, so upon substituting Eq. (41) into (C1) we obtain

$$S_0 = \tfrac{1}{2}f_1^2(f-i)^2\left[\frac{\alpha}{M\omega_D^2}\right]^2\left[\frac{\hbar}{M\omega_0}\right]\frac{\omega_D}{\omega_0} . \tag{C2}$$

In the following we set $f = i+1$. Using Eqs. (27), (33f), (26), (41), (42), and (C2) we obtain

$$\left|\sum_\kappa \mathscr{L}_{\kappa,i+1,i}\Delta_\kappa\right|^2 = 4\left[\frac{f_2}{f_1}\right]^2(i+1)(2i+1)^2 S_0^3(\hbar\omega_D)^2\frac{\omega_D}{\omega_0}\left[1+(2i+1)S_0\frac{\omega_D}{\omega_0}\right] . \tag{C3}$$

The second term in large parentheses in Eq. (C3) arises from the second term in Eq. (27). In our application S_0 is much less than 1; therefore, we can omit the second term in Eq. (27). Similarly, we obtain

$$\sum_\kappa |\mathscr{L}_{\kappa,i+1,i}|^2 = 2(f_2/f_1)(i+1)(2i+1)^2 S_0^2(\hbar\omega_D)^2\omega_D/\omega_0 , \tag{C4}$$

$$2\sum_\kappa \mathscr{L}_{\kappa,i+1,i}\sum_\lambda \mathscr{L}_{\lambda,i+1}\Delta_\lambda = 8(f_2/f_1)^2(i+1)(2i+1)S_0^2(\hbar\omega_D)^2\omega_D/\omega_0 , \tag{C5}$$

$$\left|\sum_\kappa \mathscr{M}_{\kappa,i+1,i}\right|^2 = 4(f_2/f_1)^2(i+1)S_0(\hbar\omega_D)^2\omega_D/\omega_0 . \tag{C6}$$

Substituting Eqs. (C3)–(C6) into Eq. (33b) we obtain the result given in Eq. (45).

APPENDIX D: VALIDITY OF THE SADDLE-POINT APPROXIMATION

The integral for the spectral band shape is similar to the nonradiative transition rate integral, Eq. (34), but with the nonadiabatic operator replaced by the dipole moment operator.[4] The resulting band shape is given by

$$I(\pm\omega) = \int_{-\infty}^\infty e^{\pm i\omega t + g(it)}dt . \tag{D1}$$

The saddle-point approximation for the transition rate is the first term in an asymptotic expansion in the sense defined by Poincaré.[16] In order for the first term to be a good approximation to the integral, the second term must be much smaller. The expansion for an integral of the form in Eq. (D1) has been worked out by Hoare for the case when the function $g(z)$ and its derivatives are of the order of N where N is the asymptotic expansion parameter and is presumed large.[17] In our case the relevant asymptotic parameter is p, defined in Eq. (38) in the average acoustic frequency approximation. The ratio of the second term in the asymptotic expansion to the first term must be much less than 1. Using Hoare's result, we obtain

$$\frac{1}{8}\left|\frac{g^{(4)}(z_0)}{[g''(z_0)]^2} - \frac{5[g^{(3)}(z_0)]^2}{3[g''(z_0)]^3}\right| \ll 1 . \tag{D2}$$

In the average acoustic frequency approximation, the derivatives of g are

$$g^{(2n)}(z_0) = \omega_D^{2n}P, \quad n \geq 1 \tag{D3}$$

$$g^{(2n+1)}(z_0) = \omega_D^{2n+1}P, \quad n \geq 1 \tag{D4}$$

where $P = (p^2+x^2)^{1/2}$. Substituting (D3) and (D4) in (D2), we obtain

$$\frac{1}{8p}\left|1 - \frac{5}{3}\left[\frac{p}{P}\right]^2\right| \ll 1 . \tag{D5}$$

From (D5) we see that the second term in the expansion is less than $\frac{1}{12}$ the first term if $|p|$ is greater than 1, independently of the value of x [$= S_0/\sinh(\tfrac{1}{2}\beta\hbar\omega_D)$]. We also see that the second term is less than $\frac{1}{8}$ the first term if x is greater than 1. In fact the expansion is asymptotic in the parameter P so that the approximation becomes better if either x or p becomes large.

In the case of nonradiative transitions, $|p| > 1$, so the criterion is satisfied whatever the value of S_0. In fact $|p| \gg 1$ is required for the Born-Oppenheimer approximation to be valid.

For radiative transitions, however, the saddle-point approximation is not good. For radiative transitions,

$$p = -(\omega_{fi}\pm\omega)/\omega_D , \tag{D6}$$

where the positive sign is for emission and the negative sign is for absorption at frequency ω. The range of values of p which are of interest (that is, values corresponding to frequencies within the spectral band) is then

$$p = S_0 \pm \frac{\Delta\omega}{2\omega_D} , \tag{D7}$$

where $\Delta\omega$ is the bandwidth. Since S_0 typically is much less than 1, both $|p|$ and x will be much less than 1 so that conditions (D5) cannot be satisfied for values of p which correspond to frequencies lying within a spectral band.

*Present address: BDM Corporation, McLean, VA 22102.

[1]D. J. Pastine, D. J. Edwards, H. D. Jones, C. T. Richmond, and K. Kim, in *High Pressure Science and Technology,* edited by K. D. Timmerhaus and M. S. Barber (Plenum, New York, 1979), Vol. 2.

[2]E. T. Toton (unpublished).

[3]J. H. Van Vleck, Phys. Rev. 59, 730 (1941).

[4]Yu. E. Perlin, Usp. Fiz. Nauk 80, 553 (1963) [Sov. Phys.—Usp. 6, 542 (1963)].

[5]S. H. Lin, J. Chem. Phys. 65, 1053 (1976).

[6]See, for example, Yu. E. Perlin in Ref. 4.

[7]R. C. O'Rourke, Phys. Rev. 91, 265 (1953).

[8]J. N. Plendl, in *Optical Properties of Solids,* edited by S. Nudelman and S. S. Mitra (Plenum, New York, 1969), pp. 310ff.

[9]K. Huang and A. Rhys, Proc. R. Soc. London, Ser. A 204, 406 (1950).

[10]M. Lax, J. Chem. Phys. 20, 1752 (1952).

[11]D. R. Hardesty and P. C. Lysne, Sandia Laboratories Report No. SLA-74-0165, 1974 (unpublished).

[12]Typically less than 0.02% per kbar for the optically active internal modes of nitromethane.

[13]M. Born and K. Huang, *Dynamical Theory of Crystal Lattices* (Oxford University Press, London, 1954), Sec. 4.

[14]Y. de Longueville, C. Fauquignon, and H. Moulard, in *Proceedings of the Sixth Symposium (International) on Detonation, 1976* (U.S. GPO, Washington, D.C., 1976), pp. 105ff.

[15]H. Kono and S. H. Lin, J. Chem. Phys. 78, 2607 (1983); 79, 2748 (1983).

[16]H. Jeffreys and B. S. Jeffreys, *Methods of Mathematical Physics,* 3rd ed. (Cambridge University Press, Cambridge, England, 1956), Chap. 17.

[17]M. R. Hoare, J. Chem. Phys. 52, 5695 (1970).